Accepted Manuscript

Particulate emission from the gasification and pyrolysis of biomass: Concentration, size distributions, respiratory deposition-based control measure evaluation

Zhiyi Yao, Siming You, Yanjun Dai, Chi-Hwa Wang

PII: S0269-7491(17)34907-2

DOI: 10.1016/j.envpol.2018.07.126

Reference: ENPO 11430

To appear in: *Environmental Pollution*

Received Date: 30 November 2017

Revised Date: 27 July 2018

Accepted Date: 28 July 2018

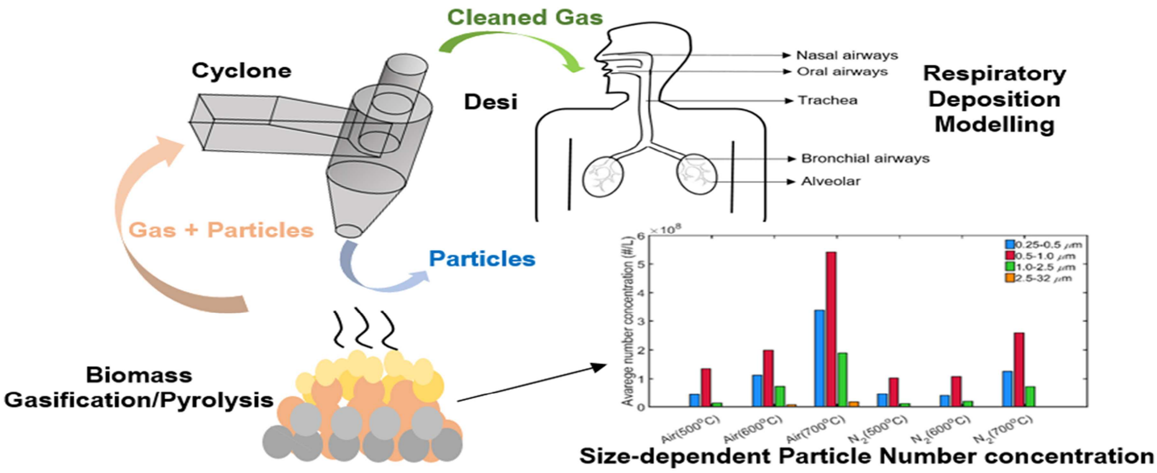

Cleaned Gas
Cyclone
Desi
Nasal airways
Oral airways
Trachea
Bronchial airways
Alveolar
Respiratory Deposition Modelling
Gas + Particles
Particles
Biomass Gasification/Pyrolysis
Avarege number concentration (#/L)
0.25-0.5 μm
0.5-1.0 μm
1.0-2.5 μm
2.5-32 μm
Air(500°C)
Air(600°C)
Air(700°C)
N2(500°C)
N2(600°C)
N2(700°C)
Size-dependent Particle Number concentration

Particulate Emission from the Gasification and Pyrolysis of Biomass: Concentration, Size Distributions, Respiratory Deposition-based Control Measure Evaluation

Zhiyi Yao[1,2†], Siming You[1#†], Yanjun Dai[3], and Chi-Hwa Wang[2*]

1 NUS Environmental Research Institute, National University of Singapore, Singapore

2 Department of Chemical and Biomolecular Engineering, National University of Singapore, Singapore

3 School of Mechanical Engineering, Shanghai Jiao Tong University, Shanghai, China

Current address: Division of Systems, Power & Energy, School of Engineering, University of Glasgow, UK

† Authors contribute equally to this work.

Resubmitted to
Environmental Pollution
July 2018

*Corresponding Author. Tel: +65 65165079; Fax: +65 67791936;
Email: chewch@nus.edu.sg (C. H. Wang)

Abstract

Gasification and pyrolysis technologies have been widely employed to produce fuels and chemicals from solid wastes. Rare studies have been conducted to compare the particulate emissions from gasification and pyrolysis, and relevant inhalation exposure assessment is still lacking. In this work, we characterized the particles emitted from the gasification and pyrolysis experiments under different temperatures (500, 600, and 700 ^oC). The collection efficiencies of existing cyclones were compared based on particle respiratory deposition. Sensitivity analysis was conducted to identify the most effective design parameters. The particles emitted from both gasification and pyrolysis process are mainly in the size range 0.25-1.0 μm and 1.0-2.5 μm. Particle respiratory deposition modelling showed that most particles penetrate deeply into the last stage of the respiratory system. At the nasal breathing mode, particles with sizes ranging from 0.25 to 1.0 μm account for around 91%, 74%, 76%, 90%, 84%, and 79% of the total number of particles that deposit onto the last stage in the cases of 500 ^oC gasification, 600 ^oC gasification, 700 ^oC gasification, 500 ^oC pyrolysis, 600 ^oC pyrolysis, and 700 ^oC pyrolysis, respectively. At the oral breathing mode, particles with sizes ranging from 0.25 to 1.0 μm account for around 92%, 77%, 79%, 91%, 86%, and 81% of the total number of particles that deposit onto the last stage in the six cases, respectively. Sensitivity analysis showed that the particle removal efficiency was found to be most sensitive to the cyclone vortex finder diameter (D_0). This work could potentially serve as the basis for proposing health protective measures against the particulate pollution from gasification and pyrolysis technologies.

Keywords: Gasification; Pyrolysis; Biomass Waste; Particle Emission; Control Measure

Capsule

A particle respiratory deposition-based cyclone design scheme is proposed for health protective measures against the particulate pollution from gasification and pyrolysis technologies.

1 Introduction

Application of waste biomass for energy production is receiving increasing attention because of the renewability and carbon neutrality features of biomass. Among the plethora of biomass-to-energy technologies, gasification and pyrolysis are considered as two of the most efficient ways to produce fuels and chemicals from biomass (Ong et al., 2015). During the gasification process, carbonaceous feedstock is converted into fuel gas, hydrocarbons, and a small amount of solid residue (*i.e.* biochar and ash) in an oxygen-deficient environment (You et al., 2017b). Pyrolysis is a thermochemical decomposition of organic material in the absence of oxygen and its major products include pyrolytic oil and biochar (Kan et al., 2016).

Biomass gasification and pyrolysis are not emission-free technologies. Thermochemical treatment of biomass was found to be one of the most important sources of $PM_{2.5}$ (particles of an aerodynamic diameter smaller than 2.5 μm) in both developed and developing countries (Glasius et al., 2006; Johnson, 2016; Saarikoski et al., 2008; Ward and Lange, 2010; Zhang et al., 2010). Several previous works have been devoted to characterizing the particulate emissions of gasification and pyrolysis. For example, the effects of feedstock moisture content on the $PM_{2.5}$ emission of a semi-gasified cookstove were investigated and $PM_{2.5}$ emission factors were found to decrease with the increase of moisture content (Huangfu et al., 2014). The particulate emissions at three locations of a fixed bed, downdraft gasifier were measured to determine the particle removal effectiveness of packed-bed filter (Hamilton et al., 2014). In the study, particle mass concentrations (PMCs) were found to be approximately 75 mg/Nm^3 in the pre-filtered producer gas and were reduced by 99% by the packed-bed filter to about 1 mg/Nm^3. A nine-stage cascade impactor was used to investigate the size distribution of particles from the gasification of municipal solid waste (MSW) (Shiota et al., 2017). The results showed that most of the particles were fine particles. $PM_{2.5}$ emission from gasification and melting of MSW accounted for 2.5% of total $PM_{2.5}$ emissions from all sorts of thermal treatment of MSW in Japan. Trace metals emission and size distribution of PM generated from biomass gasification were reported in several studies (Min et al., 2016; Nzihou and Stanmore, 2013; Pudasainee et al., 2014). The emission of potassium- and sodium-containing compounds during rapid birchwood pyrolysis was also studied (Davidsson et al., 2002). The results showed that the alkali emission per unit mass for small particles was higher than that for large ones and this tendency increased with temperature. A systematic study was conducted to characterize the emission of trace elements (e.g., As, Cu, Cr, Ni, V, Co, Cd, and Pb) generated from a two-stage pyrolysis/combustion reactor system (Liaw et al., 2016). The study indicated that particles producedfrom the combustion of volatiles produced in situ from the pyrolysis stage were smaller than 1 μm, and had a uni-modal distribution with a fine mode diameter of 0.043 μm.

Particulate emissions could potentially pose two adverse effects on the practical deployment of gasification and pyrolysis systems. First, particles could cause fouling, reduce system efficiency, contaminate the producer gas which affects the subsequent power generation and syngas upgrading processes (Hamilton et al., 2014; Wang et al., 2011; Woolcock and Brown, 2013). It was designated that the PM_{10} and PM_5 concentrations in syngas should be lower than 50 mg/m^3 and 30 mg/m^3, respectively, for internal combustion engine and gas turbine, while the PM concentration should be lower than 0.02 mg/m^3 for methanol synthesis (Woolcock and Brown, 2013). Second, gasification is a technology that is well suitable for decentralized application in terms of energy efficiency and economic feasibility (Buragohain et al., 2010;

You et al., 2016b). The decentralized application of the gasification technology in modern cities means the proximity of gasification systems to the public and residential communities. This imposes strict requirements on its emission control and management because elevated outdoor particle concentrations pose a potential health concern, especially for fine particles such as $PM_{2.5}$ that could penetrate deeply into the human respiratory system (Happo et al., 2013; Jalava et al., 2012; Moller and Loft, 2010; Naeher et al., 2007; You et al., 2016a). Our recent study also showed that elevated outdoor $PM_{2.5}$ may lead to increased household energy use and corresponding household carbon footprint by changing the energy utilization mode (e.g., more air-conditioner and purifier use) (You et al., 2017a).

Therefore, it is necessary to propose effective preventive and control measures towards particulate emissions from gasification and pyrolysis, which is highly contingent upon the understanding of the mechanisms and characteristics of particulate emission. Rare studies have been conducted to analyze the influences of operating conditions (e.g., gasification agents and temperature) towards time-resolved particulate emissions. In addition, possible particle formation mechanisms for gasification and pyrolysis are still lacking. In this work, we compared the particle removal efficiencies of existing cyclones with different configurations based on particle respiratory deposition. Sensitivity analysis was conducted to identify the most effective design parameters. This work could potentially serve as the basis for proposing health protective measures against the particulate pollution from gasification and pyrolysis technologies.

2 Materials and Methods

2.1 Experiments and Emission Calculation

2.1.1 System and instrumentation

To explore the fundamental mechanisms governing the particulate emission of the thermo-chemical processes, experiments were conducted in a lab-scale reactor (capacity: *ca*. 1g/min). A schematic diagram of the experimental setup is shown in Figure 1. The aerosol from experiments was guided into a fume hood for diluting and exhaust cooling. An aerosol spectrometer (GRIMM 1.109) was used to measure particle number concentrations (PNCs) in the fume hood. Another aerosol spectrometer was placed outside of the fume hood to measure the background PNCs. The aerosol spectrometers measured particles in the size range between 0.25 and 32 μm at an interval of 6 seconds. The duration of each sampling was about 30 min. A flask was used for tar condensation and retaining. Air and nitrogen were used as the agent for the gasification and pyrolysis experiments, respectively and the agent flow rates were fixed at 300 mL/min using a mass flow controller. 15g of feedstock was used for each experiment. For gasification experiment, the equivalence ratio (ER) was fixed as 15% during 30 minutes of experiment. $ER = \left(\frac{F_{air}}{F_s}\right) / \left(\frac{F_{air}}{F_s}\right)_{Stoichiometric}$ where F_{air} is the inlet air mass flow rate, F_s is the biomass feeding rate. Three temperatures (i.e. 500, 600, and 700 ^{o}C) were tested both for the gasification and pyrolysis experiments. The reactor was heated by electrical heater and the temperature was controlled by Programmable Logic Controller (PLC). Woodchips were used as the feedstock whose proximate, ultimate compositions were given in Table 1.

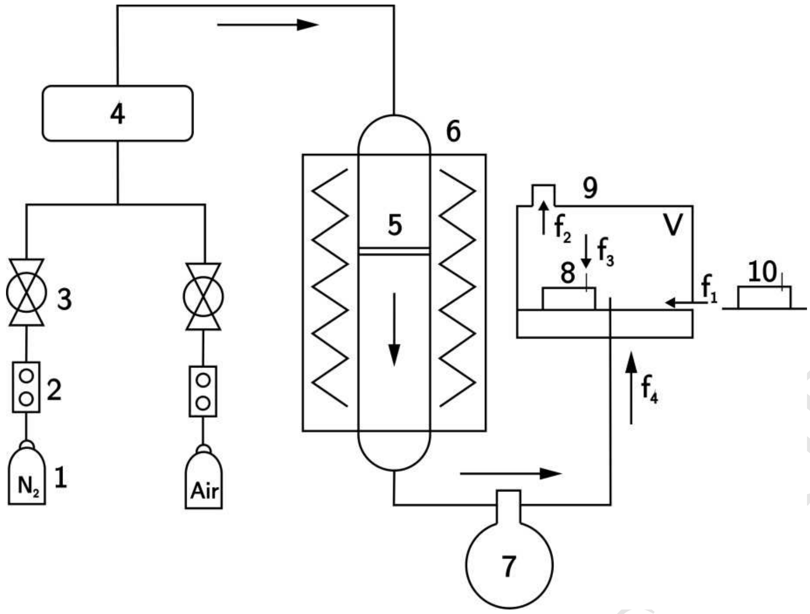

Figure 1. A schematic diagram of experimental setup. 1 Gas cylinder, 2 Mass flow controller, 3 Valve, 4 Gas mixer, 5 Gasifier reactor, 6 Heater, 7 Flask, 8 Aerosol spectrometer, 9 Fume hood, 10 Aerosol spectrometer.

Table 1. Feedstock composition.

Proximate analysis (dry basis, wt. %)	
Moisture	8.2-8.5
Volatiles	67.8-69.2
Fixed carbon	16.2-17.5
Ash	6.2-6.3
Ultimate analysis (wt. %)	
Carbon	43.3-44.2
Hydrogen	5.4-6.1
Oxygen	41.6-42.5
Nitrogen	0.9-2.1
Sulfur	0.5-1.0

2.1.2 Particulate emission calculation

The particle number concentration, PNC_{it} (#/L), was backward estimated from the concentration data based on the mass balance model

$$(\mathrm{f}_1 C_{\mathrm{ot}} - \mathrm{f}_2 C_{\mathrm{it}} - \mathrm{f}_3 C_{\mathrm{it}} + \mathrm{f}_4 PNC_{\mathrm{it}})\Delta t = (C_{\mathrm{i(t+\Delta t)}} - C_{\mathrm{it}})V \tag{1}$$

where $\Delta t = 6$ s is the sampling interval. C_{ot} (#/L) and C_{it} (#/L) are the PNC outside and inside the fume hood at the time t. C_{ot} corresponds to the measurements of the aerosol spectrometer outside the fume hood. $C_{\mathrm{i(t+\Delta t)}}$ (#/L) is the PNC inside the fume hood at the time $t + \Delta t$. C_{it} and $C_{\mathrm{i(t+\Delta t)}}$ correspond to the measurements of the aerosol spectrometer inside the fume hood. $V = 1.09 \times 10^3$ (L) is the volume of the fume hood space. f_1 (L/s), $\mathrm{f}_2 = 300$ (L/s), $\mathrm{f}_3 = 2 \times 10^{-2}$ (L/s), and f_4 (L/s) are the air flow rates entering the fume hood from outsides, exiting the fume hood, entering the aerosol spectrometer, and entering the fume hood from the reactor, respectively (Figure 1). We have $\mathrm{f}_1 + \mathrm{f}_4 = \mathrm{f}_2 + \mathrm{f}_3$. The PNC was

$$PNC_{\mathrm{it}} = \left[\frac{(C_{\mathrm{i(t+\Delta t)}} - C_{\mathrm{it}})V}{\Delta t} - \mathrm{f}_1 C_{\mathrm{ot}} + \mathrm{f}_2 C_{\mathrm{it}} + \mathrm{f}_3 C_{\mathrm{it}}\right] / \mathrm{f}_4 \tag{2}$$

We do not consider particle deposition because it is negligible compared to the ventilation effect.

2.2 Gas cyclone design based on respiratory deposition modelling

Cyclones have been considered as an economical approach for particle removal in gasification systems. Different types of cyclones (e.g., Stairmand cyclone, Lapple cyclone, German Z cyclone, and Southern Research Institute (SRI) cyclones II and III) are available and differentiated in terms of their geometrical configuration. A schematic diagram of cyclone is given in Figure 2. In this work, we compared the particle removal efficiencies of existing cyclones with different configurations based on particle respiratory deposition. Sensitivity analysis was conducted to identify the most effective design parameters. The results could be used to facilitate the design of cyclone for gasification and pyrolysis.

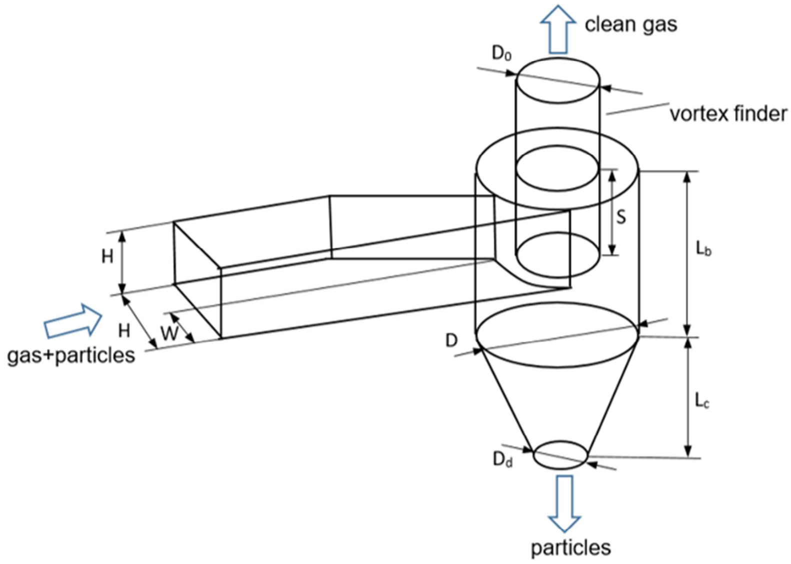

	C-20	C-25	C-30	C-35	C-40	C-45
D (mm)	20	25	30	35	40	45
Common parameters	D/D_0=2.23, H/D=0.48, W/D=0.22, S/D=0.62, (L_b+L_c)/D=2, L_b/D=1, L_0/D=2					

Figure 2. A schematic diagram of cyclone geometry and design parameters for different types of cyclones. (D: cyclone body diameter; D_0: cyclone vortex finder diameter,; D_d: cyclone bottom diameter, H: height of cyclone inlet slit,, L_b: height of cylindrical part of cyclone,; L_c: height of conical part of cyclone,; S: vortex finder length,; W: width of cyclone inlet slit,)

2.2.1 Particle removal by cyclone

The removal efficiency of the cyclones could be fitted with a linear function (Lidén and Gudmundsson, 1997) as:

$$\ln\left(\frac{E}{1-E}\right) = \mathrm{W}_0 + \mathrm{W}_1 Z \tag{3}$$

where the dimensionless parameter Z is calculated by

$$\mathrm{Z} = \frac{\sqrt{C_{cmd}(d_{ae})}d_{ae}}{\sqrt{C_{cmd}(d_{ae,50})}d_{ae,50}} - 1 \tag{4}$$

where $d_{ae} = d_e(\frac{\rho_p}{\rho_0 C_{cmd}(d_{ae})})^{1/2}$ is the aerodynamic diameter with d_e being the equivalent volume diameter and C_{cmd} being Cunningham correction factor, C_{cmd} is related to the particle Knudsen number Kn and is calculated by

$$C_{cmd} = 1 + Kn(A + B \times e^{-C/Kn}) \quad (5)$$

Where $Kn = \frac{2\lambda}{d_e}$, $A = 1.257$, $B = 0.40$, $C = 1.10$, and $\lambda = 80\ nm$ is the particle mean free path (Friedlander, 2000). $d_{ae,50}$ is the cut-off aerodynamic diameter and calculated by Muschelknautz's model (Hoffmann and Stein, 2002)

$$d_{ae,50} = x_{fact,ae}\sqrt{\frac{18\mu_g(0.9Q_v)}{2\pi(\rho_p - \rho_g)v_{\theta CS}^2(L_b + L_c - S)}} \quad (6)$$

where L_b (m) is the height of cylindrical part of cyclone, L_c (mm) is the height of conical part of cyclone, $x_{fact,ae}$ is the correction factor and it normally falls within the range of 0.9~1.4. In this study $x_{fact,ae}$ was chosen to be 1.2. Q_v (L/min) is the volumetric flow rate. S (m) is the vortex finder length, μ_g (kg/(m·s) is the gas dynamic viscosity. $v_{\theta CS}$ (m/s) is the spin velocity near the wall

$$v_{\theta CS} = v_{\theta w}(D/D_0)/(1 + \frac{fS_f v_{\theta w}\sqrt{\frac{D}{D_0}}}{2Q_v}) \quad (7)$$

where $f = 0.314Re^{-0.25}$ is the wall friction factor (Karagoz and Avci, 2005). $Re = \frac{\rho_g u_{in}(D - D_0)/2}{\mu_g}$. D (m) is the cyclone body diameter, D_0 (m) is the cyclone vortex finder diameter. $v_{\theta w}$ (m/s) is the geometrical mean rotational velocity

$$v_{\theta w} = u_{in}R_{in}/(\alpha R_m) \quad (8)$$

where u_{in} (m/s) is the average gas velocity at cyclone inlet. R_{in} (m) is the radial position of the centre of the inlet, $R_{in} = D/2 - W/2$. R_m (m) is the geometric mean radius. $R_m = \sqrt{(D/2)(D_0/2)}$. α is the first regression coefficient, $\alpha = 0.04$. S_f (m^2) is the friction surface estimated by

$$S_f = \frac{\pi}{4}[D^2 - D_0^2 + 4(DL_b + D_0S) + (D + D_d)\sqrt{4L_c^2 + (D - D_d)^2}] \quad (9)$$

with D_d (m) being the cyclone bottom diameter.

2.2.2 Respiratory deposition modelling

The cyclone design is based on particle respiratory deposition modelling. (You et al., 2017c) summarized the existing particle deposition models (Chan et al., 1980; Cheng, 2003; Cohen and Asgharian, 1990; Kim and Fisher, 1999; Kim and Iglesias, 1989; Zamankhan et al., 2006; Zhang et al., 2008). As shown in Figure S1, the airways were divided into five stages for modelling submicron particle deposition in the human respiratory system [oral (stage 1) and nasal (stage 1) airways, trachea (stage 2), bronchial airways from B1 to B6 (stage 3) and from B7 to B15 (stage 4), and the rest of airways (stage 5)]. For modelling supermicron particle deposition in the human respiratory system, the airways were divided into four stages [oral (stage 1) and nasal (stage 1) airways, trachea (stage 2), the bronchial airways from B1 to B19 (stage 3), and the rest of airways (stage 4)]. The boundary between submicron particles and supermicron particles is defined as 1 micrometer. The compiled models and parameters for particle respiratory deposition modelling is given in Table S1-S3 (please see the Supplementary Material).

In this study, six types of commonly used cyclones (i.e. C-20, C-25, C-30, C-35, C-40, and C-45) were compared in terms of their effects on mitigating particle respiratory deposition. The corresponding design parameters of the cyclones are shown in Figure 2 (Sagot et al., 2017). A case without cyclone was also considered for the purpose of comparison.

2.3 Sensitivity analysis

Parameter investigation was conducted to explore the relationships between the design parameters (X/X_0, where X means the ratio of design parameter to cyclone diameter D, X_0 means original ratio of design parameter to cyclone diameter D.) of cyclone geometry and the particle removal efficiency of the cyclone. Each design parameter was investigated by varying the parameter from 50% to 150% of its nominal value while keeping the rest of parameters unchanged as nominal values.

3 Results and Discussion

3.1 Particulate emission comparison between gasification and pyrolysis

3.1.1 Particulate emission dynamics in terms of PNC_{it}

The variation of PNCs under different operating conditions is given in Figure 3. Generally, PNCs increase by 3.4 times with temperature increasing from 500 ^{o}C to 700 ^{o}C. Particles emitted from the gasification process are around 1.1 times more than particles emitted from the pyrolysis process. The particles emitted from both the gasification and pyrolysis process are mainly in the size range 0.25-1.0 μm, suggesting a potential exposure risk to intermediate-mode particles (particles with sizes ranging from 0.1 μm to 1.0 μm (Kohli and Mittal, 2015)). The results are consistent with the study by (Shiota et al., 2017) and most of the particles emitted from a gasification plant were found to be less than 3 μm.

The emission-initiating temperatures (the temperature where explicit emissions are observed) are around 200 and 400 ^{o}C for gasification and pyrolysis, respectively. The lower emission-initiating temperature for gasification than that for pyrolysis should be related to the fact that partial oxidation takes place in the gasfication process with the existence of oxygen. The effects of temperature on particulate emissions were investigated by several researchers. Nam et al., (2010) studied the influence of ambient temperature on PM emissions from gasoline-powered vehicles. They found that in general, particulate emissions doubled for every 20 °F drop in ambient temperature. Nosek et al., (2014) analyzed the effects of primary combustion air temperature on the heat performance and particulate emissions of burning biomass. No obvious trend was observed on the particulate emissions with increasing primary combustion air temperature. However, to the best of our knowledge, none of them has reported the relationship between the initiation of particulate emission and temperature. The PNC profiles generally exhibit a unimodal feature for the case of 600 ^{o}C for both gasification and pyrolysis, while the PNC profiles exhibit a bimodal feature for the cases of 500^{o}C and 700 ^{o}C, which corresponds to two emission peaks for both the gasification and pyrolysis. At 500 ^{o}C, upon the initiation of the experiments, gasification or pyrolysis reactions take place and syngas is released together with fine particles, which leads to the first emission peak. As the reactions going on, solid organic material is converted into gaseous species and particle porosity increases gradually to such a level that further particle fragmentation takes place, which leads to the second emission peak. At 600 ^{o}C, porosity increases faster due to the relatively high teamperature compared to the case of 500 ^{o}C, which causes the overlap of these two peaks. At 700 ^{o}C, temperature is high enough and thermal stress will cause further breakage of the ash in the gasification process. For pyrolysis, particle fragmentation rate is relatively slow without the existence of oxygen. Hence, in the gasification process the particles continue to be emitted at lower rate after reaching the first emission peak but in the pyrolysis process the second emission initiates after a short period. Real-time particulate emission from incineration of solid waste under high temperature (>850 ^{o}C) was monitored (Derrough et al., 2013) and a small secondary emission peak was also observed . However, no explanation has been provided for this phenomena in the study.

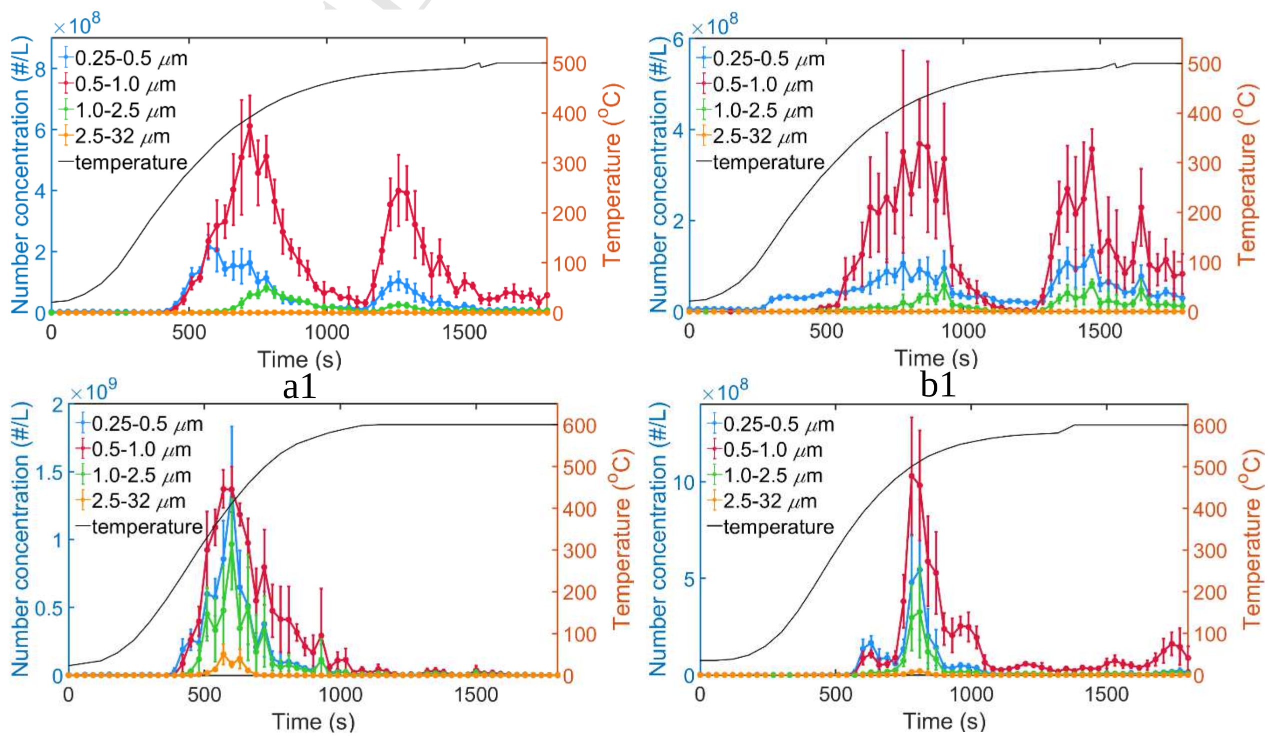

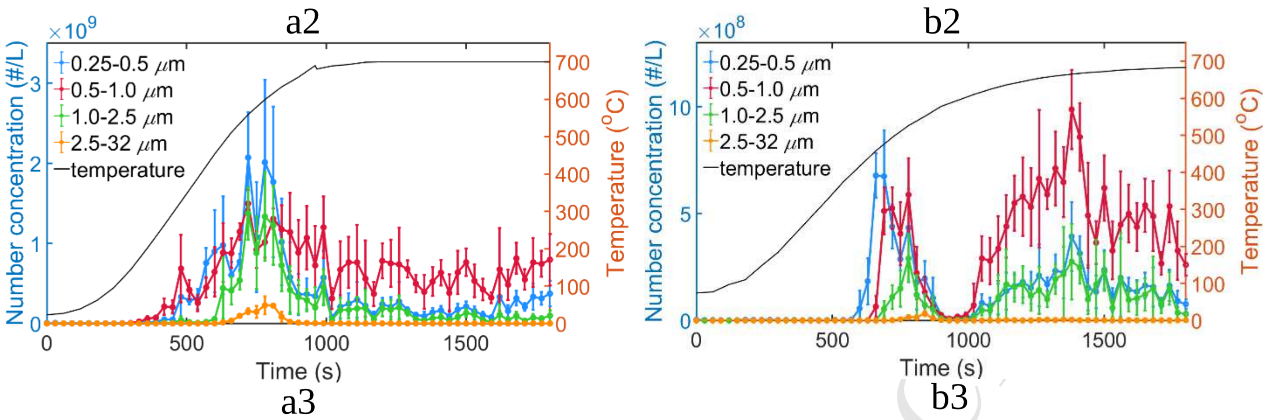

Figure 3. The variation of nc_{it} under different operating conditions. (a1: gasification, 500°C; a2: gasification, 600°C; a3: gasification, 700°C; b1: pyrolysis, 500°C; b2: pyrolysis, 600°C; b3: pyrolysis, 700°C).

3.1.2 Particle size distributions

The size-dependent average particle number and volume concentrations of different cases are given in Figure 4a and 4b, respectively. The measured PNCs including all size ranges are 1.92×10^{8}, 3.90×10^{8}, 1.09×10^{9}, 1.59×10^{8}, 1.68×10^{8}, 4.57×10^{8} #/L for the case of 500 °C gasification, 600 °C gasification, 700 °C gasification, 500 °C pyrolysis, 600 °C pyrolysis, and 700 °C pyrolysis, respectively. The measured particle volume concentrations (PVCs) including all size ranges are 7.95×10^{-12}, 4.80×10^{-10}, 1.10×10^{-9}, 6.05×10^{-11}, 9.98×10^{-11}, 3.15×10^{-10} m^3/L for the case of 500 °C gasification, 600 °C gasification, 700 °C gasification, 500 °C pyrolysis, 600 °C pyrolysis, and 700 °C pyrolysis, respectively. Since higher operaing temperature favors higher chemical reaction rates, both PNCs and PVCs increase with increasing temperature in both gasification and pyrolysis processes. In addition, gasification emits more particles compared with pyrolysis, mainly due to the factor that high-speed partial oxidation reactions take place in the gasification process, which serves to convert carbon from solid phase to gas phase and causes more significant particle fragmentation and emission. For the case of 700^{o}C, the number concentration of particles emitted from gasification is 170%, 110 %, 161%, 772% higher than that emitted from pyrolysis for the size bins of 0.25 - 0.5, 0.5 - 1.0, 1.0 - 2.5, 2.5 - 32.0 μm, respectively. The particles with sizes ranging from 0.5 to 1.0 μm account for the biggest proportion of emitted particles in terms of number concentration, which is 70.09%, 50.84%, 49.86%, 64.41%, 63.77%, 56.37% for the cases of 500^{o}C gasification, 600^{o}C gasification, 700^{o}C gasification, 500^{o}C pyrolysis, 600^{o}C pyrolysis, and 700^{o}C pyrolysis, respectively. However, the particles with sizes ranging from 1.0 to 2.5 μm account for the biggest proportion of emitted particles according to their size-dependent volume concentrations, which is 39.60%, 51.94%, 58.14%, 43.08%, 53.16%, 65.29% for the cases of 500^{o}C gasification, 600^{o}C gasification, 700^{o}C gasification, 500^{o}C pyrolysis, 600^{o}C pyrolysis, and 700^{o}C pyrolysis, respectively. These results suggest a great concern about exposure to intermediate-accumulation-mode particles (particles with sizes ranging from 0.1 μm to 2.5 μm (Kohli and Mittal, 2015)). A bimodal particle size distribution at 700^{o}C incineration was observed and it was found that the maximum number concentration being at about 80 nm and the minor one at 40 nm (Maguhn et al., 2003). The incineration process should be able to emit particles smaller than that from gasification and pyrolysis, because it could provide enough oxygen to convert biomass to finer particles by a higher temperature. Similarly, the $PM_{2.5}$ emitted from incineration was found to consist of about 99% of submicrometer sized particles and about 65% of ultrafine particles were $PM_{0.1}$ (Buonanno et al., 2009). The normalized particle number size distributions in dN/dlogDp and particle volume size distributions in dV/dlogDp are shown in Figure S2 in the Supplementary Material.

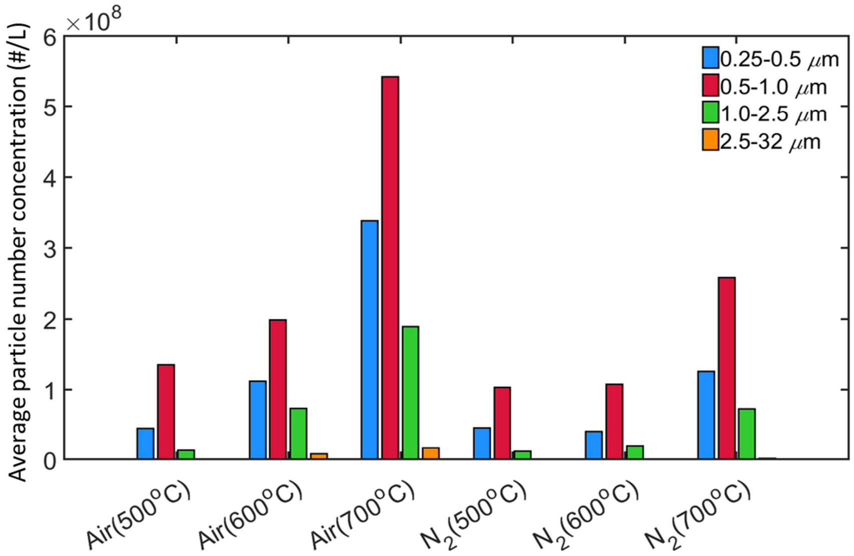

a

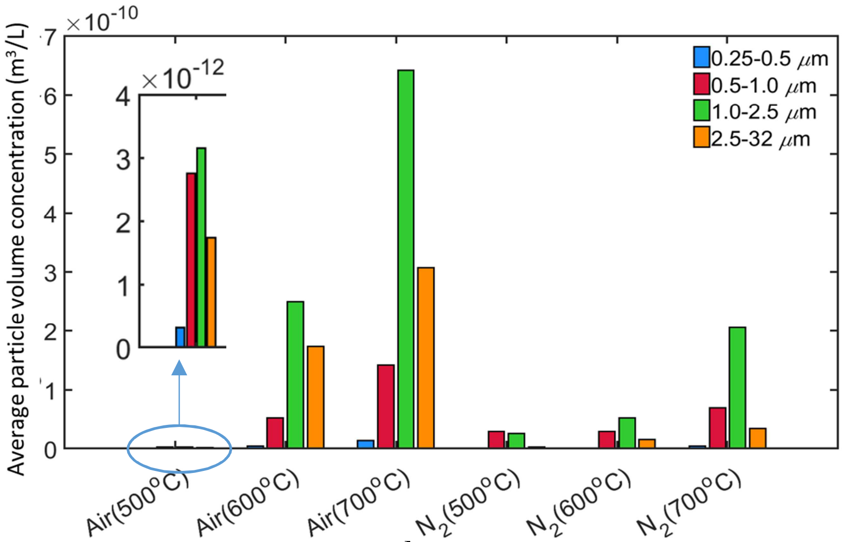

b

Figure 4. a: Size-dependent average PNCs under different reaction conditions.
b: Size-dependent average PVCs under different reaction conditions.

3.1.3 Particle deposition on human respiratory system

Figure 5 shows the results of particle number deposition modes in the human respiratory system. The particle number size distributions (PNSDs) are calculated by assuming that all the emitted particles are directly inhaled by human respiratory system. It was found that most particles could penetrate deeply into the last stage of the respiratory system, *i.e.*, the 5th and 4th stages for submicron particles and supermicron particles, respectively. At the nasal breathing mode, particles with sizes ranging from 0.25 to 1.0 μm account for around 91%, 74%, 76%, 90%, 84%, and 79% of the total number of particles that deposit onto the last stage in the cases of 500 ^{o}C gasification, 600 ^{o}C gasification, 700 ^{o}C gasification, 500 ^{o}C pyrolysis, 600 ^{o}C pyrolysis, and 700 ^{o}C pyrolysis, respectively. At the oral breathing mode, particles with sizes ranging from 0.25 to 1.0 μm account for around 92%, 77%, 79%, 91%, 86%, and 81% of the total number of particles that deposit onto the last stage in the six cases, respectively. The trend of particle deposition through nasal and oral breathing modes is roughly the same. However, significant more submicron particles deposit onto the first stage for a nasal breathing mode than an oral breathing mode, which indirectly causes around 10.8% more submicron particles to penetrate deeply to the last stage for the oral breathing mode. Considering that the greatest health concern is related to the deposition of particles into the deep lung system (Cassee et al., 2002; Ferin et al., 1990), the nasal breathing mode could potentially serve to mitigate human exposure to aerosols. The detailed data of PNSDs in the human respiratory system is listed in Table S4 in the Supplementary Material. Table S5 lists the results of particle volume distributions in the human respiratory system. By taking into account of particle volumes, particles with sizes ranging from 1.0 to 2.5 μm account for the biggest proportion of the total volume of particles that deposit onto the last stage of human respiratory system, which is different from the results of particle number deposition. At the nasal breathing mode, particles with sizes ranging from 1.0 to 2.5 μm account for around 53%, 55%, 62%, 58%, 63%, and 74% of the total volume of particles that deposit onto the last stage in the cases of 500 ^{o}C gasification, 600 ^{o}C gasification, 700 ^{o}C gasification, 500 ^{o}C pyrolysis, 600 ^{o}C pyrolysis, and 700 ^{o}C pyrolysis, respectively. At the oral breathing mode, particles with sizes ranging from 1.0 to 2.5 μm account for around 51%, 55%, 62%, 55%, 62%, and 73% of the total volume of particles that deposit onto the last stage in the six cases, respectively.

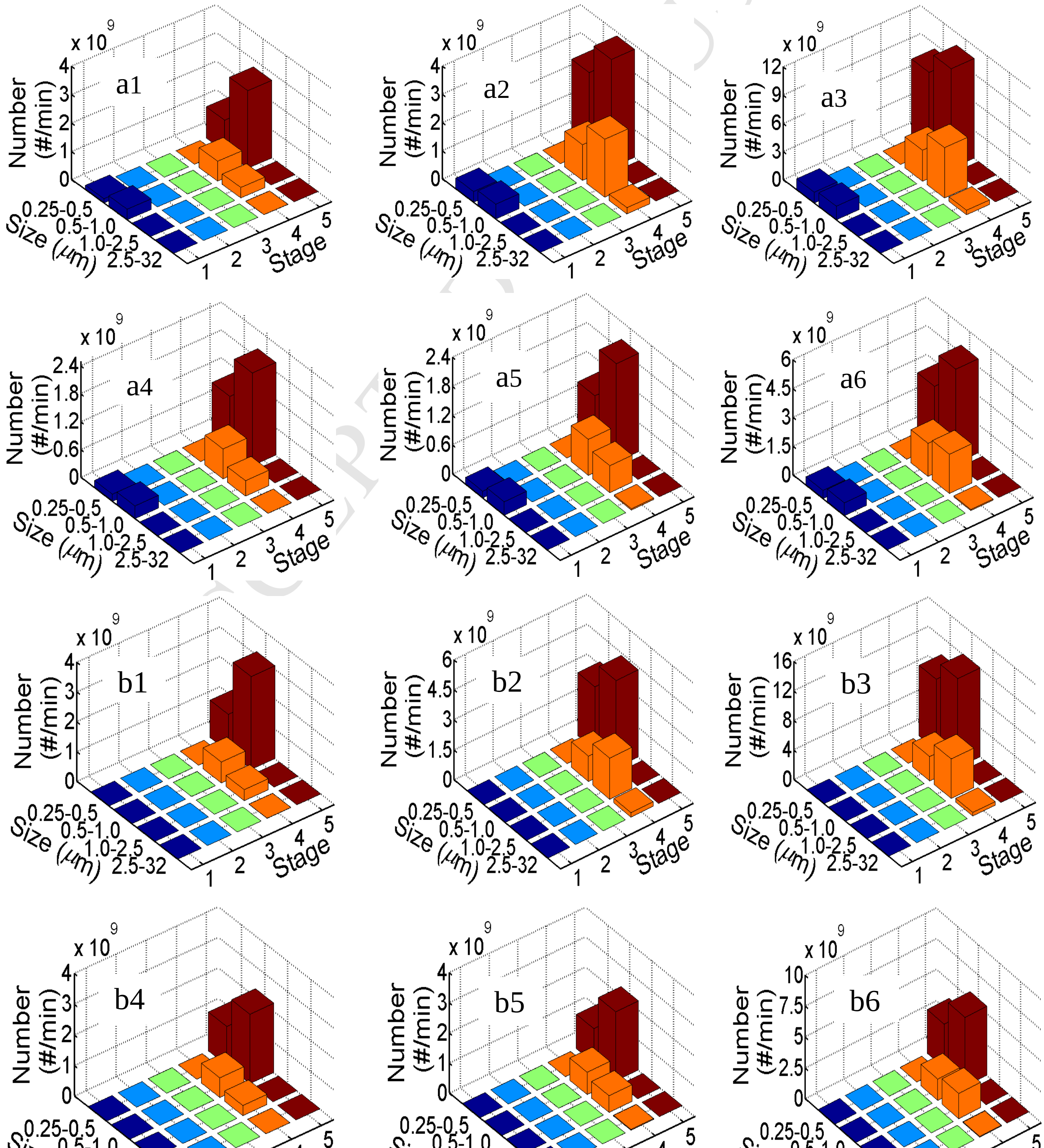

Figure 5. Particle deposition on human respiratory system through:
Nasal airway: a1: gasification, 500°C; a2: gasification, 600°C; a3: gasification, 700°C; a4: pyrolysis, 500°C; a5: pyrolysis, 600°C; a6: pyrolysis, 700°C;
Oral airway: b1: gasification, 500°C; b2: gasification, 600°C; b3: gasification, 700°C; b4: pyrolysis, 500°C; b5: pyrolysis, 600°C; b6: pyrolysis, 700°C.

3.2 Comparison of cyclone removal efficiency based on respiratory modelling

Particle-removal ability of cyclone was investigated based on the results of particle deposition modelling. The removal efficiency of particle number was calculated as the following:

$$e_n = \frac{\sum_i \mathrm{PN}_{oi} - \mathrm{PN}_{ci}}{\sum_i \mathrm{PN}_{oi}} \tag{10}$$

The removal efficiency of particle volume is calculated as the following:

$$e_v = \frac{\sum_i (\mathrm{PN}_{oi} \times V_{oi} - \mathrm{PN}_{ci} \times V_{ci})}{\sum_i (\mathrm{PN}_{oi} \times V_{oi})} \tag{11}$$

where PN_{oi}(#/min) is the number of particles within size range i deposited on the human respiratory system in the case without a cyclone, V_{oi} (m^3/#) is the volume of a particle within size range i deposited on the human respiratory system in the case without a cyclone. PN_{ci} (#/min) is the number of particles within size range i deposited on the human respiratory system after the exhaust gas passing through a cyclone. V_{ci} (m^3/#) is the volume of a particle within size range i deposited on the human respiratory system after the exhaust gas passing through a cyclone. The particle removal efficiencies in different stages of human respiratory system were calculated by assuming a flowrate of 52 L/min and the results are shown in Figure 6. Compared with submicron particles, supermicron particles could be more effectively removed by the cyclones. In all the cases, the removal efficiency of submicron particle number reaches its peak at the last stage of human respiratory system, while the removal efficiency of supermicron particle number reaches its peak at the stage of Bronchial airways. At each stage in the respiratory system, the removal efficiency of particle number decreases with the cyclone diameter (*D*) increasing from 20 mm to 45 mm. At the nasal breathing mode, the average removal efficiency of submicron particle number among all the stages of human respiratory system is 15.16%, 4.41%, 1.90%, 1.07%, 0.70% and 0.51% by cyclone C-20, C-25, C-30, C-35, C-40 and C-45, respectively, in the gasification process. The average removal efficiency of supermicron particle number among all the stages of human respiratory system is 90.13%, 68.92%, 47.56%, 28.93%, 15.65% and 8.09% by cyclone C-20, C-25, C-30, C-35, C-40 and C-45, respectively, in the gasification process. The average removal efficiency of submicron particle number among all the stages of human respiratory system is 15.83%, 4.54%, 1.94%, 1.08%, 0.71%, 0.51% by cyclone C-20, C-25, C-30, C-35, C-40 and C-45, respectively, in the pyrolysis process. The average removal efficiency of supermicron particle number among all the stages of human respiratory system is 86.35%, 58.60%, 34.71%, 18.23%, 9.07%, 4.80% by cyclone C-20, C-25, C-30, C-35, C-40 and C-45, respectively, in the pyrolysis process. Similar trends could be observed in Figure S3, which shows the removal efficiencies of particle volume in each stage of the human respiratory system as a function of cyclone diameter.

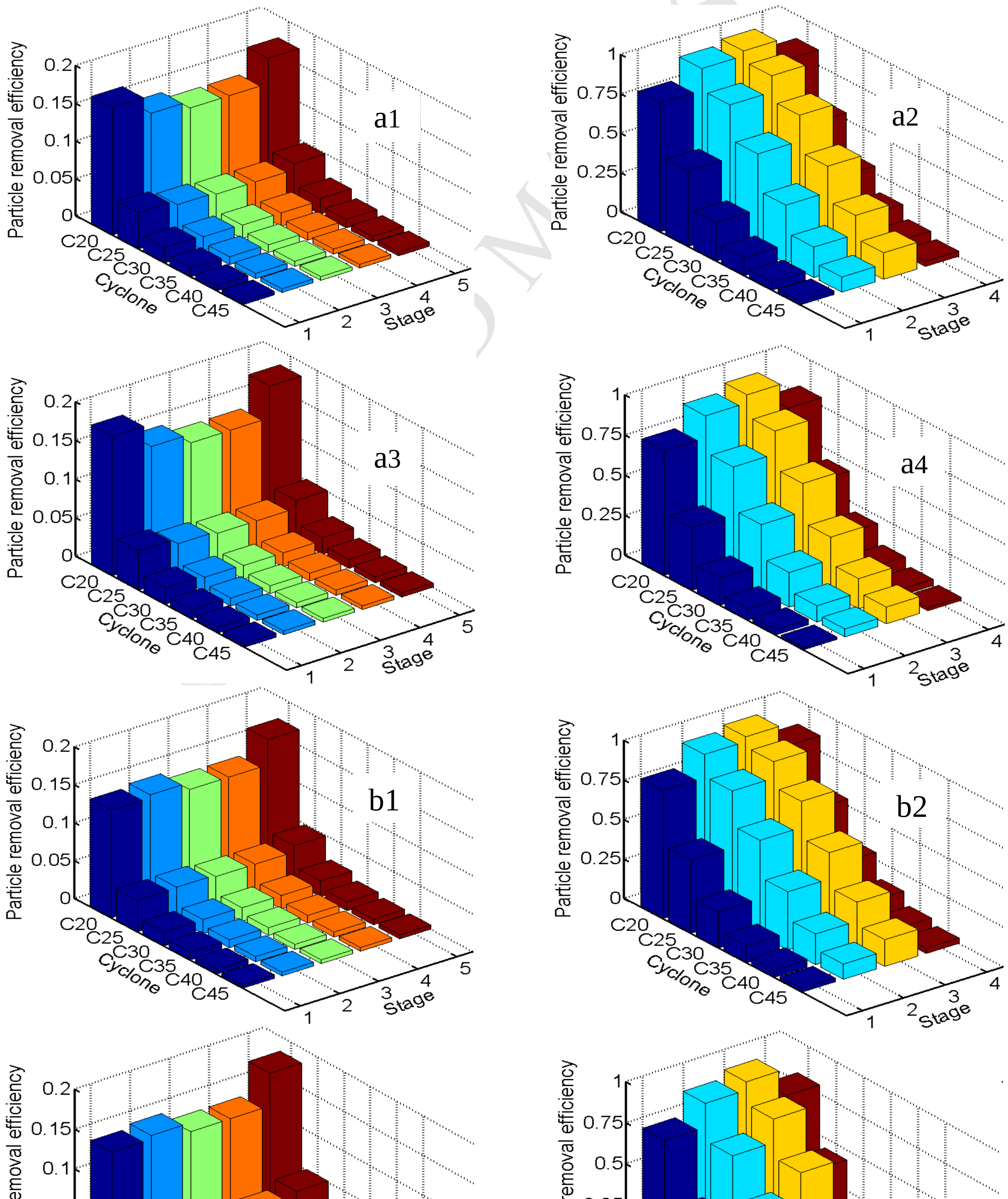
a1
a2
a3
a4
b1
b2
Particle removal efficiency
Cyclone
Stage
C20
C25
C30
C35
C40
C45
0
0.05
0.1
0.15
0.2
0.25
0.5
0.75
1
2
3
4
5

b3 b4

Figure 6. Removal efficiency of particle number in different stages of human respiratory system: Nasal breathing model: a1: sub-micro particles (gasification), a2: microparticles (gasification), a3: sub-micro particles (pyrolysis), a4: micro particles (pyrolysis);
Oral breathing model: b1: sub-micro particles emitted (gasification), b2: microparticles (gasification), b3: sub-micro particles (pyrolysis), b4: microparticles (pyrolysis).

We present in Figure 7 the removal efficiencies of particle number for different cyclones as a function of the flow rate. Although the total reduced number of submicron particles associated with the gasification process is double that associated with the pyrolysis process, the removal efficiencies of particle number for different cyclones show the similar trends in the cases of both gasification and pyrolysis. For the gasification process, with the flow rate increasing from 24 to 116 L/min, the removal efficiency of particle number increases from 10.64%, 3.60%, 1.23%, 0.54%, 0.31% and 0.21% to 80.01%, 56.33%, 35.94%, 23.41%, 15.54% and 10.17% for cyclone C-20, C-25, C-30, C-35, C-40 and C-45, respectively. For the pyrolysis process, with the flow rate increasing from 24 to 116 L/min, the removal efficiency of particle number increases from 7.39%, 2.17%, 0.80%, 0.41%, 0.26% and 0.18% to 79.59%, 56.51%, 34.19%, 20.27%, 12.18% and 7.35% for cyclone C-20, C-25, C-30, C-35, C-40 and C-45, respectively. For the practical applications, C-20 has the best particle removal ability. The results suggest that increasing flowrate has a positive effect on the particle removal efficiency of the cyclone, while increasing cyclone diameter has a negative effect on the particle removal efficiency of the cyclone. Similar results were found by (Sagot et al., 2017). An increase of the particle removal efficiency with the increase of the flow rate was attributed to the stronger centrifugal force created by the higher flowrates. A reduction of the particle removal efficiency with the increase of the cyclone diameter was because of the fact that reducing cyclone diameter could lead to an increase of the internal velocity, thus producing higher centrifugal forces and improving the particle removal efficiency. The removal efficiencies for submicron and supermicron particles were plotted separately in Figure S4 in the Supplementary Material. The removal efficiencies for supermicron particles are higher compared to submicron particles because removal efficiency generally increases with increasing particle size, which is also inherent to the calculation of cyclone efficiency.

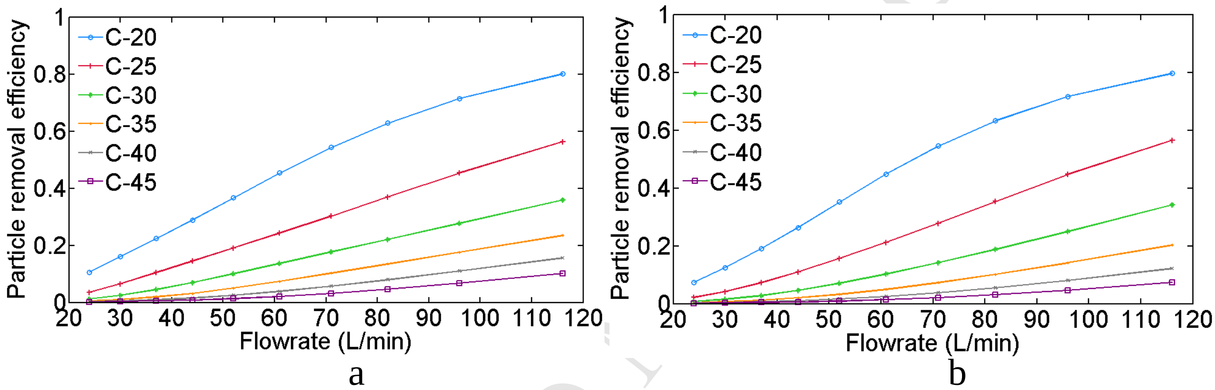

Figure 7. Removal efficiency of particle number of different cyclones under different air flowrate. (a: gasification, b: pyrolysis).

3.3 Sensitivity analysis

The effects of design parameters on the removal efficiency of particle number are shown in Figure 8. Both gasification and pyrolysis show the similar trends of the removal efficiency of particle number under different design parameters of the cyclone. For the gasification process, the removal efficiency of submicron particles decreases from 67.49%, 48.25%, 46.70%, and 24.77% to 3.35%, 7.06%, 6.35%, and 10.95%, as X/X_0 increases from 0.5 to 1.5 for the cases of D_0/D, H/D, W/D and S/D, respectively, which means that increasing D_0, H, W and S has a negative effect on the removal efficiency. Although the removal efficiency of submicron particles increases from 15.25%, 12.98% and 16.94% to 16.91%, 18.90%, and 16.94%, as X/X_0 increases from 0.5 to 1.5, for L_b/D, L_c/D, and L_0/D, respectively, L_b, L_c, and L_0 have negligible effect on the cyclone removal efficiency, as they generally fall along the horizontal line. Hence, the variation of L_b, L_c, and L_0 may have a limited effect on changing cyclone removal efficiency. The similar trends could be observed in the removal efficiencies of supermicron particles under different design parameters. However, the removal efficiency of supermicron particles is significantly higher than that of submicron particles. Among these seven parameters, the particle removal efficiency is found to be most sensitive to D_0, which suggests that the most effective way of modifying the cyclone design is on the change of D_0. Similarly, reducing D_0 has the most significantly positive effect on reducing particle volume deposition in the human respiratory system, as shown in Figure S5 in the Supplementary Material. In addition, as the value of D_0/D decreases, the slope of D_0/D tends to remain constant for submicron particles, while the slope of D_0/D tends to increase for supermicron particles. The results show that there is still a large potential of removing submicron particles from the system by decreasing D_0/D. However, decreasing D_0/D would reach its limit of reducing deposited supermicron particles because the removal efficiency of supermicron particles is approaching 100%.

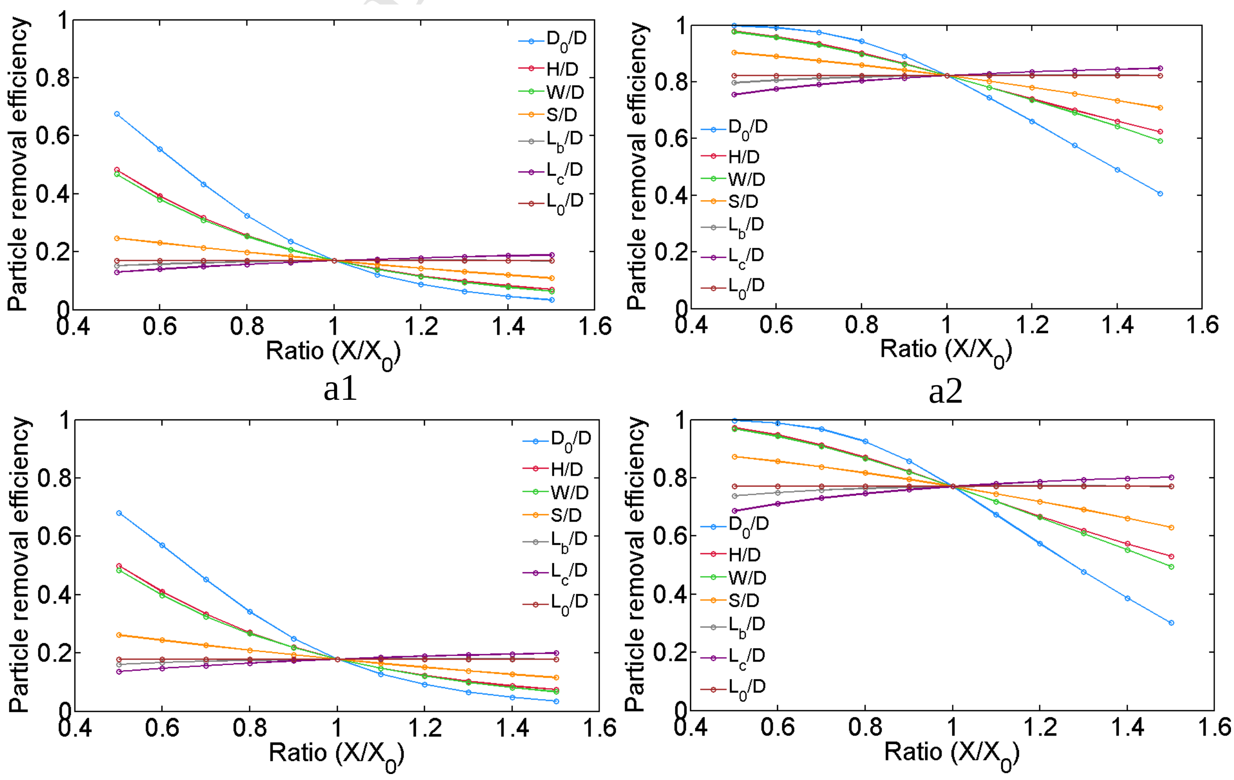

b1 b2

Figure 8. Removal efficiency of particle number under different design parameters: a1: submicron particle (gasification); a2: supermicron particle (gasification); b1: submicron particle (pyrolysis); b2: supermicron particle (pyrolysis).

4 Conclusions

In this work, we characterized the particulate emission potential of the gasification and pyrolysis process. We compared the particle removal efficiencies of existing cyclones with different configurations based on particle respiratory deposition. Sensitivity analysis was conducted to identify the most effective design parameters. Generally, PNCs increase by 3.4 times with temperature increasing from 500 ^{o}C to 700 ^{o}C. Particles emitted from the gasification process are around 1.1 times more than particles emitted from the pyrolysis process. The particles emitted from both gasification and pyrolysis process are mainly particles within the size range 0.25-1.0 μm and particles within the size range 1.0-2.5 μm. The emission-initiating temperatures for gasification and pyrolysis were found to be around 200 and 400 ^{o}C, respectively. The PNC profiles generally exhibit a single mode feature for the case of 600 ^{o}C for both gasification and pyrolysis, while the PNC profiles exhibit a bimodal feature for the case of 500 and 700 ^{o}C, respectively. Particle respiratory deposition modelling showed that most particles penetrate deeply into the last stage of the respiratory system, *i.e.* the 5th and 4th stages for submicron particles and supermicron particles, respectively. To minimize total particle number deposited onto the human respiratory system, gas cyclone diameter (*D)* should be small. Sensitivity analysis showed that the cyclone collection efficiency was found to be most sensitive to D_0, which suggests that the most effective way of modifying cyclone design would be the one associated with changing D_0. The results from this study could not only provide information for setting up the emission standards for gasifiers, but also serve as the basis for controlling the particulate pollution from gasification and pyrolysis technologies.

Acknowledgements

This research program is funded by the National Research Foundation (NRF), Prime Minister's Office, Singapore under its Campus for Research Excellence and Technological Enterprise (CREATE) program Grant Number R- 706-001-101-281, National University of Singapore. We also acknowledge the technical support of Shen Ye and Bian Zhoufeng (National University of Singapore) on the project.

Appendix A. Supplementary Material

Additional Data could be found in the Supplementary Material.

References

Buonanno, G., Ficco, G., Stabile, L., 2009. Size distribution and number concentration of particles at the stack of a municipal waste incinerator. Waste Management 29, 749-755.
Buragohain, B., Mahanta, P., Moholkar, V.S., 2010. Biomass gasification for decentralized power generation: The Indian perspective. Renewable and Sustainable Energy Reviews 14, 73-92.
Cassee, F.R., Muijser, H., Duistermaat, E., Freijer, J.J., Geerse, K.B., Marijnissen, J.C., Arts, J.H., 2002. Particle size-dependent total mass deposition in lungs determines inhalation toxicity of cadmium chloride aerosols in rats. Application of a multiple path dosimetry model. Archives of toxicology 76, 277-286.
Chan, T.L., Schreck, R.M., Lippmann, M., 1980. Effect of the laryngeal jet on particle deposition in the human trachea and upper bronchial airways. Journal of Aerosol Science 11, 447-459.
Cheng, Y.S., 2003. Aerosol deposition in the extrathoracic region. Aerosol Science & Technology 37, 659-671.
Cohen, B., Asgharian, B., 1990. Deposition of ultrafine particles in the upper airways: an empirical analysis. Journal of Aerosol Science 21, 789-797.
Davidsson, K., Stojkova, B., Pettersson, J., 2002. Alkali emission from birchwood particles during rapid pyrolysis. Energy & Fuels 16, 1033-1039.
Derrough, S., Raffin, G., Locatelli, D., Nobile, P., Durand, C., 2013. Behaviour of nanoparticles during high temperature treatment (Incineration type), Journal of Physics: Conference Series. IOP Publishing, p. 012047.
Ferin, J., Oberdörster, G., Penney, D., Soderholm, S., Gelein, R., Piper, H., 1990. Increased pulmonary toxicity of ultrafine particles? I. Particle clearance, translocation, morphology. Journal of Aerosol Science 21, 381-384.
Friedlander, S.K., 2000. Smoke, Dust, and Haze: Fundamentals of Aerosol Dynamics. Topics in Chemical Engineering. Oxford University Press, New York.
Glasius, M., Ketzel, M., Wahlin, P., Jensen, B., Monster, J., Berkowicz, R., Palmgren, F., 2006. Impact of wood combustion on particle levels in a residential area in Denmark. Atmospheric Environment 40, 7115-7124.
Hamilton, J.E., Adams, J.M., Northrop, W.F., 2014. Particulate and Aromatic Hydrocarbon Emissions from a Small-Scale Biomass Gasifier–Generator System. Energy & Fuels 28, 3255-3261.

Happo, M.S., Uski, O., Jalava, P.I., Kelz, J., Brunner, T., Hakulinen, P., Maki-Paakkanen, J., Kosma, V.M., Jokiniemi, J., Obernberger, I., Hirvonen, M.R., 2013. Pulmonary inflammation and tissue damage in the mouse lung after exposure to PM samples from biomass heating appliances of old and modern technologies. Sci Total Environ 443, 256-266.

Hoffmann, A.C., Stein, L.E., 2002. Computational fluid dynamics, Gas Cyclones and Swirl Tubes. Springer, pp. 123-135.

Huangfu, Y., Li, H., Chen, X., Xue, C., Chen, C., Liu, G., 2014. Effects of moisture content in fuel on thermal performance and emission of biomass semi-gasified cookstove. Energy for Sustainable Development 21, 60-65.

Jalava, P.I., Happo, M.S., Kelz, J., Brunner, T., Hakulinen, P., Mäki-Paakkanen, J., Hukkanen, A., Jokiniemi, J., Obernberger, I., Hirvonen, M.-R., 2012. In vitro toxicological characterization of particulate emissions from residential biomass heating systems based on old and new technologies. Atmospheric Environment 50, 24-35.

Johnson, D.R., 2016. Nanometer-sized emissions from municipal waste incinerators: A qualitative risk assessment. J Hazard Mater 320, 67-79.

Kan, T., Strezov, V., Evans, T.J., 2016. Lignocellulosic biomass pyrolysis: A review of product properties and effects of pyrolysis parameters. Renewable and Sustainable Energy Reviews 57, 1126-1140.

Karagoz, I., Avci, A., 2005. Modelling of the Pressure Drop in Tangential Inlet Cyclone Separators. Aerosol Science and Technology 39, 857-865.

Kim, C.S., Fisher, D.M., 1999. Deposition characteristics of aerosol particles in sequentially bifurcating airway models. Aerosol Science & Technology 31, 198-220.

Kim, C.S., Iglesias, A.J., 1989. Deposition of inhaled particles in bifurcating airway models: I. Inspiratory deposition. Journal of Aerosol Medicine 2, 1-14.

Kohli, R., Mittal, K.L., 2015. Developments in Surface Contamination and Cleaning, Vol. 1: Fundamentals and Applied Aspects. William Andrew.

Liaw, S.B., Rahim, M.U., Wu, H., 2016. Trace Elements Release and Particulate Matter Emission during the Combustion of Char and Volatiles fromIn SituBiosolid Fast Pyrolysis. Energy & Fuels 30, 5766-5771.

Lidén, G., Gudmundsson, A., 1997. Semi-empirical modelling to generalise the dependence of cyclone collection efficiency on operating conditions and cyclone design. Journal of aerosol science 28, 853-874.

Maguhn, J.r., Karg, E., Kettrup, A., Zimmermann, R., 2003. On-line analysis of the size distribution of fine and ultrafine aerosol particles in flue and stack gas of a municipal waste incineration plant: effects of dynamic process control measures and emission reduction devices. Environmental science & technology 37, 4761-4770.

Min, J., Nam, S.-B., Kim, N.-R., Kim, D.-J., Yoon, Y.-S., Park, S.-N., Gu, J.-H., 2016. A study on the characteristics of particulate matter in the syngas produced from the waste gasification with cleaning systems for energy utilization. Journal of Material Cycles and Waste Management.

Moller, P., Loft, S., 2010. Oxidative damage to DNA and lipids as biomarkers of exposure to air pollution. Environ Health Perspect 118, 1126-1136.

Naeher, L.P., Brauer, M., Lipsett, M., Zelikoff, J.T., Simpson, C.D., Koenig, J.Q., Smith, K.R., 2007. Woodsmoke health effects: a review. Inhal Toxicol 19, 67-106.

Nam, E., Kishan, S., Baldauf, R.W., Fulper, C.R., Sabisch, M., Warila, J., 2010. Temperature effects on particulate matter emissions from light-duty, gasoline-powered motor vehicles. Environmental science & technology 44, 4672-4677.

Nosek, R., Holubcik, M., Papucik, S., 2014. Emission controls using different temperatures of combustion air. ScientificWorldJournal 2014, 487549.

Nzihou, A., Stanmore, B., 2013. The fate of heavy metals during combustion and gasification of contaminated biomass-a brief review. J Hazard Mater 256-257, 56-66.

Ong, Z., Cheng, Y., Maneerung, T., Yao, Z., Tong, Y.W., Wang, C.-H., Dai, Y., 2015. Co-gasification of woody biomass and sewage sludge in a fixed-bed downdraft gasifier. AIChE Journal 61, 2508-2521.

Pudasainee, D., Paur, H.-R., Fleck, S., Seifert, H., 2014. Trace metals emission in syngas from biomass gasification. Fuel Processing Technology 120, 54-60.

Saarikoski, S.K., Sillanpää, M.K., Saarnio, K.M., Hillamo, R.E., Pennanen, A.S., Salonen, R.O., 2008. Impact of Biomass Combustion on Urban Fine Particulate Matter in Central and Northern Europe. Water, Air, and Soil Pollution 191, 265-277.

Sagot, B., Forthomme, A., Yahia, L.A.A., De La Bourdonnaye, G., 2017. Experimental study of cyclone performance for blow-by gas cleaning applications. Journal of Aerosol Science 110, 53-69.

Shiota, K., Tsujimoto, Y., Takaoka, M., Oshita, K., Fujimori, T., 2017. Emission of particulate matter from gasification and melting furnace for municipal solid waste in Japan. Journal of Environmental Chemical Engineering 5, 1703-1710.

Wang, X., Robbins, C., Hoekman, S.K., Chow, J.C., Watson, J.G., Schuetzle, D., 2011. Dilution sampling and analysis of particulate matter in biomass-derived syngas. Frontiers of Environmental Science & Engineering in China 5, 320-330.

Ward, T., Lange, T., 2010. The impact of wood smoke on ambient PM2.5 in northern Rocky Mountain valley communities. Environ Pollut 158, 723-729.

Woolcock, P.J., Brown, R.C., 2013. A review of cleaning technologies for biomass-derived syngas. Biomass and Bioenergy 52, 54-84.

You, S., Neoh, K.G., Tong, Y.W., Dai, Y., Wang, C.-H., 2017a. Variation of household electricity consumption and potential impact of outdoor PM 2.5 concentration: A comparison between Singapore and Shanghai. Applied Energy 188, 475-484.

You, S., Ok, Y.S., Chen, S.S., Tsang, D.C., Kwon, E.E., Lee, J., Wang, C.-H., 2017b. A Critical Review on Sustainable Biochar System through Gasification: Energy and Environmental Applications. Bioresource technology.

You, S., Tong, Y.W., Neoh, K.G., Dai, Y., Wang, C.-H., 2016a. On the association between outdoor PM 2.5 concentration and the seasonality of tuberculosis for Beijing and Hong Kong. Environmental Pollution 218, 1170-1179.

You, S., Wang, W., Dai, Y., Tong, Y.W., Wang, C.H., 2016b. Comparison of the co-gasification of sewage sludge and food wastes and cost-benefit analysis of gasification- and incineration-based waste treatment schemes. Bioresour Technol 218, 595-605.

You, S., Yao, Z., Dai, Y., Wang, C.H., 2017c. A comparison of PM exposure related to emission hotspots in a hot and humid urban environment: Concentrations, compositions, respiratory deposition, and potential health risks. Sci Total Environ 599-600, 464-473.

Zamankhan, P., Ahmadi, G., Wang, Z., Hopke, P.K., Cheng, Y.-S., Su, W.C., Leonard, D., 2006. Airflow and deposition of nano-particles in a human nasal cavity. Aerosol Science and Technology 40, 463-476.

Zhang, X., Hecobian, A., Zheng, M., Frank, N.H., Weber, R.J., 2010. Biomass burning impact on PM_{2.5} over the southeastern US during 2007: integrating chemically speciated FRM filter measurements, MODIS fire counts and PMF analysis. Atmospheric Chemistry and Physics 10, 6839-6853.

Zhang, Z., Kleinstreuer, C., Kim, C.S., 2008. Airflow and nanoparticle deposition in a 16-generation tracheobronchial airway model. Annals of Biomedical Engineering 36, 2095-2110.

- Particulate emissions of gasification and pyrolysis are compared.
- The particles from gasification and pyrolysis are mainly $PM_{0.25\text{-}1.0}$ and $PM_{1.0\text{-}2.5}$.
- Most particles penetrate deeply into the last stage of the respiratory system.
- A particle respiratory deposition-based cyclone design scheme is proposed.
- The cyclone vortex finder diameter is the most sensitive design parameter.